Progress In Electromagnetics Research C, Vol. 103, 167–176, 2020

Absorptive Filter Integrated Single Pole Double Throw Switch Using Switchable T-Shape Resonator for IoT Applications

Abdullah M. Zobilah[1, *], Noor A. Shairi[1], Zahriladha Zakaria[1], Peng W. Wong[2], Mohd K. Zahari[1], Mohammed Y. Algumaei[1], and Zayed A. Nasser[1]

Abstract—In this paper, an absorptive filter-integrated switch (FIS) using switchable T-shape resonators is presented. The FIS was made up of two absorptive T-shape resonators and integrated with single pole double throw (SPDT) switch. A simple mathematical analysis of isolation and insertion loss of filter-integrated SPDT switch is discussed. PIN diodes were used as the switching elements for the SPDT switch and to reconfigure between the band-stop and bandpass responses. The proposed absorptive FIS design could be used for internet of things (IoT) applications such as Zigbee and Bluetooth at an operation frequency of 2.45 GHz. As a result, the proposed FIS exhibited low magnitude of insertion loss and high isolation. Therefore, the key advantages of the proposed FIS design are low insertion loss, high isolation, and good return loss at both ON- and OFF-state ports.

1. INTRODUCTION

Recently, Radio Frequency (RF) and microwave devices integration have become a popular design concept. Integrated-power amplifier modulator [1], amplifier integrated with RF switch [2, 3], and integrated-filter antenna [4] are examples of such integrated devices.

Filter-integrated switch (FIS) as depicted in Figure 1 is another integrated/multifunction device. From the year 2006 onwards, numerous studies have reported filter-integrated double pole double throw (DPDT) switch [5], single pole single throw (SPST) switch [6–8], and SPDT switch [9–24]. In order to produce FISs and integrate BPF with SPDT switch in one device, several techniques have been used, such as dielectric resonators (DRs) [15], LC resonators [11], substrate integrated suspended line (SISL) [30], and common shorted stepped-impedance resonator (CSSIR) [25].

Unfortunately, all these FISs as previously mentioned suffer from different issues. Many of them have been proposed in monolithic microwave integrated-circuit (MMIC) technology [7, 8, 10, 12, 18–20, 22]. While MMICs allow for most compact designs, the conventional planar circuits exhibit greater flexibility at a lower cost. Besides, all of the previous studies except for [23] have a problem of extremely low return loss at the ports that are not switched to the antenna, or also called as OFF-state ports. The low return loss is caused by a reflection of an incoming signal back to the source. This problem should be solved as, for some applications, good voltage standing wave ratio (VSWR) for all operating ports required [23], and RF switch is preferred to mitigate the problems of multiple internal reflections existing in the RF front end, which can reduce the effect of microwave switch on the RF front end performance [25]. An absorptive feature, the ability of the device to create high return loss at the OFF-state port, was introduced in SPDT switch design [23], but required additional switch elements and a 50 Ω resistor.

Received 5 May 2020, Accepted 22 June 2020, Scheduled 6 July 2020

* Corresponding author: Abdullah Mohammed Saghir Zobilah (zobilah12@hotmail.com).
[1] Microwave Research Group (MRG), Centre for Telecommunication Research & Innovation (CeTRI), Fakulti Kejuruteraan Elektronik dan Kejuruteraan Komputer (FKEKK), Universiti Teknikal Malaysia Melaka (UTeM), Hang Tuah Jaya, Durian Tunggal, Melaka 76100, Malaysia. [2] Electrical & Electronic Engineering Department, Universiti Teknologi Petronas (UTP), Bandar Seri Iskandar, Tronoh, Perak 31750, Malaysia.

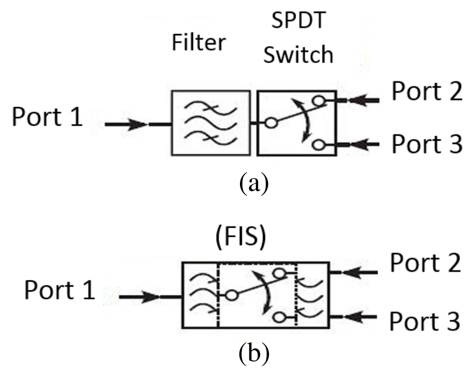

Figure 1. The diagram of the (a) conventional filter and SPDT switch, (b) filter integrated SPDT switch [9].

This paper presents the design and analysis of an absorptive filter-integrated SPDT switch using a T-shape resonator. The design is under the FIS category, which is proposed to be used for transmitting and receiving operations in time division duplex (TDD) communication. The proposed design is based on a perfectly-matched T-shape band-stop filter [26]. PIN diodes were used as switching elements to reconfigure between the band-stop and bandpass responses on coupled line ring resonators. The proposed design was demonstrated at 2.45 GHz with the performance analyses of insertion loss, return loss, and isolation.

Therefore, the proposed design resulted in many benefits, such as eliminating out-of-band signals and filtering out the spurious signal. Moreover, integrating the switchable matched band-stop to a bandpass filter with SPDT switch would result in a system miniaturisation, reduction of insertion loss, and improvement of isolation.

2. SWITCHABLE T-SHAPE RESONATOR DESIGN

The layout of the T-shape switchable resonator, as shown in Figure 2, occupies 42.2 mm × 28.4 mm area, excluding the biasing circuits. The 90° length, or $\lambda 4$, of the band-stop resonator circuit was loaded with two PIN diodes. The PIN diodes operate between 'ON' and 'OFF' states to switch from band-stop response to the bandpass filter response. The biasing for PIN diodes consisted of DC power supply, RF chokes, DC block, and 47 Ω of resistor.

The operation of this design is based on the PIN diodes acting as a switching element either 'ON' or 'OFF'. When the PIN diodes were supplied with +5 V, the PIN diodes were switched 'ON', and band-stop response was produced. When the PIN diodes were supplied with 0 V, then the PIN diodes were switched 'OFF', and bandpass response was produced.

From the simulated result as shown in Figure 3(a), the absorptive band-stop filter resonates at center frequency 2.45 GHz, where the isolation, S_{12}, was 10 dB, and the return loss, S_{11}, was 8 dB. Even if the isolation is not very high, it is enough to create very high magnitude in the FIS level. When the 90° length resonator was disconnected, the signal propagated via parallel coupled resonators K_1 and K_2 to the output at 270°. The bandpass filter was produced at the filter output when the PIN diodes were switched 'OFF'. The simulation result of the switchable resonator during bandpass response was centered at 2.45 GHz. Figure 3(b) shows the bandpass response, where the return loss (S_{11}) was 13.6 dB, and insertion loss (S_{12}) was 3.5 dB. Table 1 summarizes the simulation result of the T-shape switchable resonator.

Table 1. The simulation result of the T-SPST.

L-SPST	Bandpass response		Band-stop response	
	S_{11}	S_{12}	S_{11}	S_{12}
	13.6 dB	3.5 dB	8.0 dB	10.0 dB

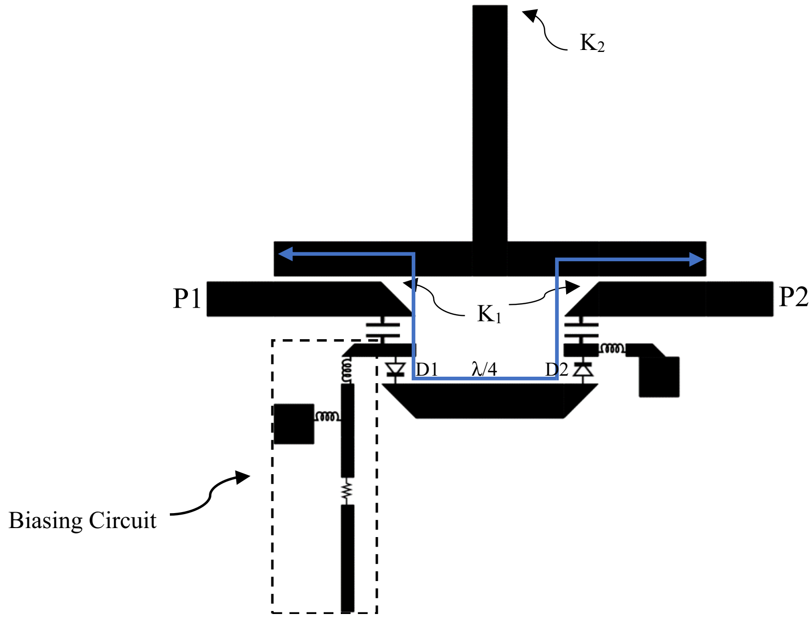

Figure 2. The diagram of the T-shape switchable resonator.

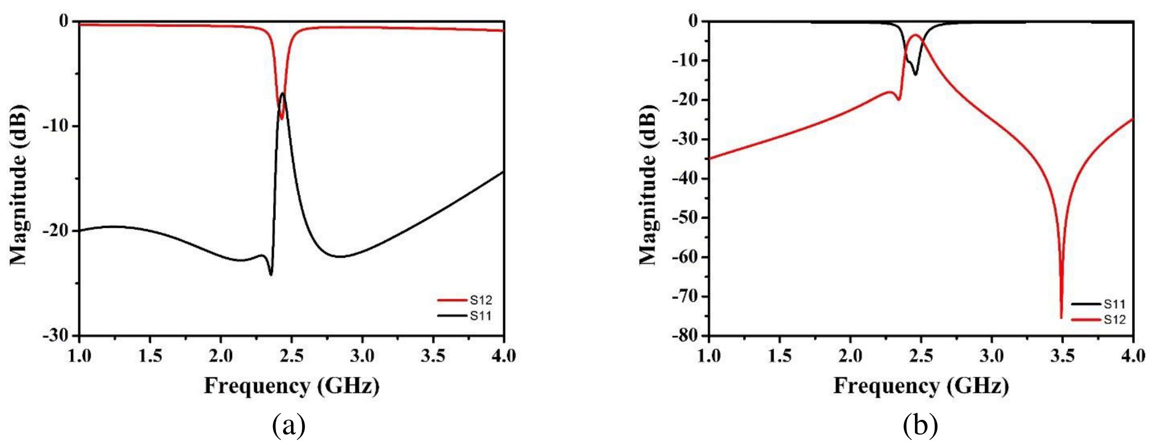

Figure 3. The simulation result of the T-shape single pole single throw (T-SPST); (a) Isolation (S_{12}) and the return loss (S_{11}); (b) Insertion loss (S_{12}) and the return loss (S_{11}).

3. MATHEMATICAL ANALYSIS OF T-SHAPE FILTER-INTEGRATED SPDT SWITCH

Figure 4 presents the circuit diagram of the proposed absorptive T-shape filter integrated SPDT switch. The following subsections discuss the mathematical analysis of the isolation and insertion loss.

3.1. The Isolation of Filter-Integrated SPDT Switch

This is a simple mathematical analysis and discussion of isolation of filter-integrated SPDT switch. The $ABCD$ matrix of the two-port network was analysed by considering OFF state PIN diodes in the T-shape switchable resonator ($R1$). Besides, the series PIN diode ($D3$) was OFF too. Hence, the $ABCD$ matrix could be as follows:

$$[T] = [\ T_{D3}\ ][\ T_{R2}\ ] = \begin{bmatrix} A & B \\ C & D \end{bmatrix} \tag{1}$$

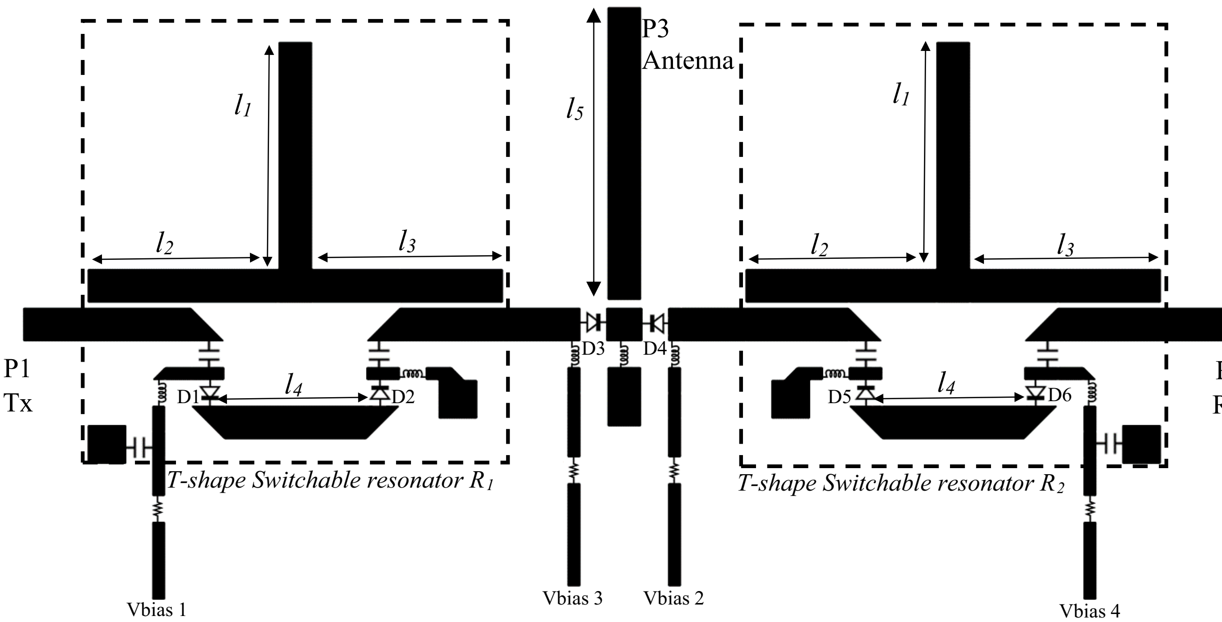

Figure 4. The diagram of the absorptive FIS using T-shape switchable resonator.

$$[\ T_{D3}\ ] = \begin{bmatrix} 1 & Z \\ 0 & 1 \end{bmatrix} = \begin{bmatrix} 1 & Rr + j\left(\omega Li - \dfrac{1}{\omega Ci}\right) \\ 0 & 1 \end{bmatrix} \tag{2}$$

$$[\ T_{R2}\ ] = \begin{bmatrix} \dfrac{Ye+Yo}{Yo-Ye} & \dfrac{2}{Yo-Ye} \\ \dfrac{2YeYo}{Yo-Ye} & \dfrac{Ye+Yo}{Yo-Ye} \end{bmatrix} \tag{3}$$

where T_{D3} is the transfer $ABCD$ matrix of series PIN diode in OFF state, R_r the PIN diode resistance during reverse bias, L the inductance of PIN diode, C the capacitance of PIN diode [27], T_{R2} the transfer $ABCD$ matrix of the symmetrical network [28], and Y_e and Y_o are the even- and odd-mode admittances, respectively. Converting the $ABCD$ matrix of Eq. (1) to S-parameter, S_{12} is expressed as

$$S_{12} = \frac{2}{A+B+C+D} \tag{4}$$

By substituting the result of Eq. (1) into Eq. (4),

$$S_{12} = \frac{2(Yo-Ye)}{2\,(Ye+Yo)+2\left(Rr+j\left(\omega Li-\dfrac{1}{\omega Ci}\right)\right)YeYo+2+\left(Rr+j\left(\omega Li-\dfrac{1}{\omega Ci}\right)\right)(Ye+Yo)+2YeYo} \tag{5}$$

For a perfectly matched system at resonance frequency: $Yo - Ye = 0$. Therefore,

$$S12 = 0$$

Or in decibel

$$|S_{12}|^2\ \text{dB} = 20\log(0) = \infty\,\text{dB} \tag{6}$$

Theoretically, it was clearly observed that infinite isolation S_{12} could be achieved if $Yo - Ye = 0$. From Eq. (6), an ideal infinite attenuation (notch) was produced. This attenuation characteristic was used to produce high isolation in T-shape filter-integrated SPDT switch.

3.2. The Insertion Loss of Filter-Integrated SPDT Switch

This is a simple analysis and discussion of insertion loss of filter-integrated SPDT switch. The $ABCD$ matrix of the two-port network was analysed by considering an ON state PIN didoes in the T-shape switchable resonator ($R2$). Besides, the series PIN diode ($D2$) was ON too. Hence, the $ABCD$ matrix could be as follows:

$$[\ T_{D2}\ ] = \begin{bmatrix} 1 & Z \\ 0 & 1 \end{bmatrix} = \begin{bmatrix} 1 & Rf + j\omega Li \\ 0 & 1 \end{bmatrix} \tag{7}$$

$$[\ T_{R1}\ ] = \begin{bmatrix} \frac{Ye+Yo}{Yo-Ye} & \frac{2}{Yo-Ye} \\ \frac{2YeYo}{Yo-Ye} & \frac{Ye+Yo}{Yo-Ye} \end{bmatrix} \tag{8}$$

$$[T] = \begin{bmatrix} 1 & Rf + j\omega Li \\ 0 & 1 \end{bmatrix} \begin{bmatrix} \frac{Ye+Yo}{Yo-Ye} & \frac{2}{Yo-Ye} \\ \frac{2YeYo}{Yo-Ye} & \frac{Ye+Yo}{Yo-Ye} \end{bmatrix} \tag{9}$$

$$[T] = \begin{bmatrix} \frac{Ye+Yo}{Yo-Ye} + \frac{2\,(Rf + j\omega Li)\,YeYo}{Yo-Ye} & \frac{2}{Yo-Ye} + \frac{(Rf + j\omega Li)\,(Ye+Yo)}{Yo-Ye} \\ \frac{2YeYo}{Yo-Ye} & \frac{Ye+Yo}{Yo-Ye} \end{bmatrix} \tag{10}$$

where R_f is the resistance of PIN diode during forward bias. Converting the $ABCD$ matrix of Eq. (10) to S-parameter, S_{13} is expressed as

$$S_{13} = \frac{2}{A+B+C+D} \tag{11}$$

$$= \frac{2(Yo-Ye)}{2\,(Ye+Yo) + 2\,(Rf + j\omega Li)\,YeYo + 2 + (Rf + j\omega Li)\,(Ye+Yo) + 2YeYo} \tag{12}$$

During bandpass operation, the PIN diodes (D) were in the ON state. In this case, the even and odd mode admittances are derived as follows [29]:

$$Yo = \frac{K_1^2}{Ys - K_2} \tag{13}$$

$$Ye = \frac{K_1^2}{Ys + K_2} \tag{14}$$

For bandpass response at resonance

$$S13 = 1$$

when

$$(Y_e - Y_o) = (1 + Y_o)(1 + Y_e) \tag{15}$$

To reach this case,

$$Y_{sub}^2 + 2K_1^2 Y_{sub} + K_1^4 = K_2(2K_1^2 + K_2) \tag{16}$$

where Y_{sub} is the characteristic impedance of the resonator $R1$. For the proposed topology, K_1 is the same during band-stop and bandpass operation. At resonance frequency, the capacitance value of K_1 is as follows:

$$K_1 = 14\,\text{pF/cm}$$

Then,

$$Y_{sub}^2 + 2\left(14 * 10^{-12}\right)^2 Y_{sub} + \left(14 * 10^{-12}\right)^4 = K_2\left(2(14 * 10^{-12})^2 + K_2\right) \tag{17}$$

$$K_2^2 + 2\left(14 * 10^{-12}\right)^2 K_2 - \left[Y_{sub}^2 + 2\left(14 * 10^{-12}\right)^2 Y_{sub} + \left(14 * 10^{-12}\right)^4\right] = 0 \tag{18}$$

To simplify the equation, let

$$Y_{sub}^2 + 2\left(14 * 10^{-12}\right)^2 Y_{sub} + \left(14 * 10^{-12}\right)^4 = A \tag{19}$$

$$2\left(14 * 10^{-12}\right)^2 = D \tag{20}$$

Therefore, Equation (18) is as follows

$$K_2^2 + DK_2 - A = 0 \tag{21}$$

Solving this equation,

$$K_2 = D \pm \sqrt{D^2 + A} \tag{22}$$

Substituting Eqs. (13), (14), & (22) into Eq. (12). Thus,

$$S_{13} = 1 = 0\,\text{dB} \tag{23}$$

Theoretically, it is clearly observed that zero insertion loss S_{13} can be achieved if $(Y_e - Y_o) = (1 + Y_o)(1 + Y_e)$. From Eq. (23), an ideal insertion loss was produced. This insertion loss characteristic was used to produce low insertion loss in the T-shape filter-integrated SPDT switch.

4. ABSORPTIVE T-SHAPE FILTER-INTEGRATED SPDT SWITCH DESIGN

Figure 4 is the diagram of the discussed design: the absorptive FIS using T-shape resonators. In particular, the FIS circuit was designed for the purpose of switching between the transmitter (Tx) mode and receiver (Rx) mode, as well as to filter both the transmitted and received signals.

For illustration, two reconfigurable T-shape resonators R1 and R2 were utilized to achieve the filter and switch performance. Besides, two PIN diodes (D3 and D4) were used to enhance the isolation between transmitter (Tx) and receiver (Rx) modes.

The resonators along with the entire FIS were symmetrically designed for both receiver arm and transmitter arm. However, in this section, only the operation of the transmitter (Tx) mode will be discussed, whereby P1 is ON-state, and P2 is OFF-state. In this mode, the RF signals propagated from Tx to the Antenna. In this condition, the PIN diodes D1 and D2 were turned OFF, thus the T-shape resonator of R1 worked as a bandpass filter. Moreover, the PIN diode of D3 was turned ON to allow the RF signals to freely pass to the Antenna. On the other hand, the PIN diodes of D5 and D6 were turned ON, thus allowing the T-shape resonator of R2 to work as a band-stop filter. Besides, the PIN diode of D4 was turned OFF to minimize the power leakage. Clearly, in this process, the band-stop response of R2 in the receiver (Rx) arm was the ultimate reason for the isolation between Tx and Rx. In addition, the bandpass response of R1 (in Tx arm) was the ultimate reason for filtering the transmitted signals. Table 2 represents the summary of the process during Rx and Tx modes of the proposed absorptive FIS at the operation frequency of 2.45 GHz.

Table 2. The process summarization of the absorptive ring FIS.

	Receiver Mode	Transmitter Mode
Vbias1& 2	+5 Volt	−5 Volt
Vbias3 & 4	−5 Volt	+5 Volt
Series PIN diode (D3)	OFF state	ON state
Series PIN diode (D4)	ON state	OFF state
Switchable Ring Resonator (R1)	Band-stop response	Bandpass response
Switchable Ring Resonator (R2)	Bandpass response	Bandstop response

Advanced Design System (ADS) software was used for the proposed FIS design performance of insertion loss, return loss, and isolation. The FIS was fabricated using an FR4 substrate with the following parameters: thickness = 1.6 mm and relative dielectric constant, $\varepsilon_r = 4.7$. The switching elements, PIN diodes, and variable capacitance diodes were from NXP with the part numbers of BAP64-02 and BB145B, respectively. The layout dimensions are as follows: $l_1 = 17.6\,\mathrm{mm}$, $l_2 = 14.8\,\mathrm{mm}$, $l_3 = 14.8\,\mathrm{mm}$, $l_4 = 11.0\,\mathrm{mm}$, $l_5 = 22.7\,\mathrm{mm}$, $w = 2.6\,\mathrm{mm}$, $S = 0.4\,\mathrm{mm}$.

5. SIMULATION AND MEASUREMENT RESULTS OF THE FIS

The fabricated device of proposed design of absorptive T-shape filter-integrated SPDT switch (FIS) is shown in Figure 5. The total size of the fabricated FIS was $91.2\,\mathrm{mm} \times 31\,\mathrm{mm}$.

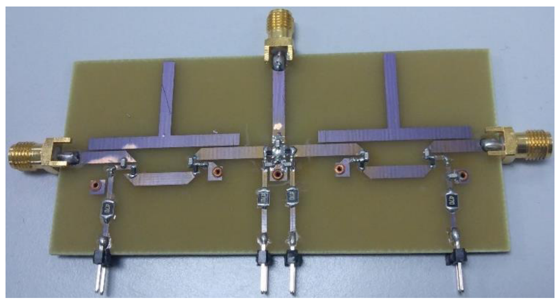

Figure 5. The prototype of the absorptive FIS using T-shape resonator.

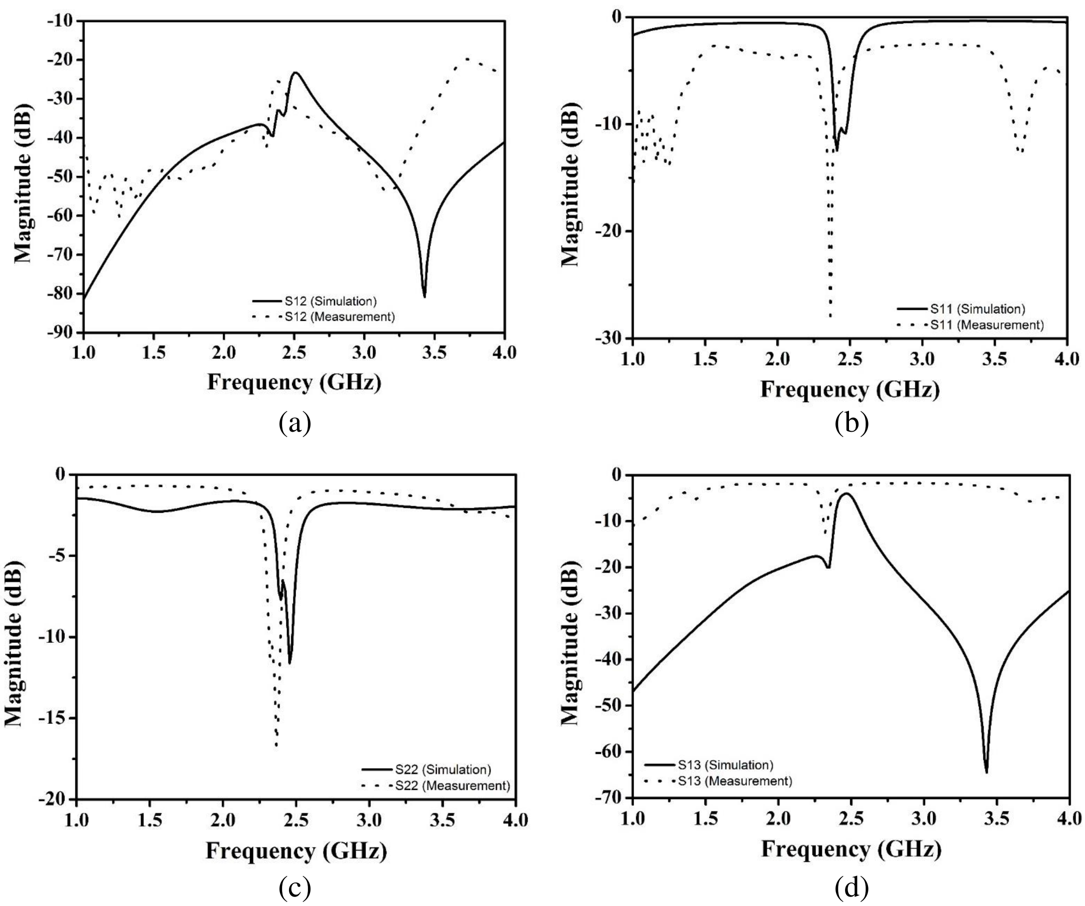

Figure 6. Simulation and measurement results of absorptive filter-integrated SPDT switch using T-shape resonator, (a) isolation (S_{12}), (b) return loss (S_{11}), (c) return loss (S_{22}) and (d) insertion loss (S_{13}).

Figure 6 indicates the simulated and measured results of the FIS, using T-shape resonator, during Tx mode, whereby P1 is ON-state, and P2 is OFF-state. Besides, the same output could be obtained for the Rx mode, as the FIS circuit was designed symmetrically. The results are as follows: isolation (Figure 6(a)), return loss of Port 1 (Figure 6(b)), return loss of Port 2 (Figure 6(c)), and insertion loss (Figure 6(d)). Furthermore, the simulated isolation (S_{12}) between the transmitter and receiver was 31 dB.

Based on the obtained isolation, the proposed FIS had the ability to isolate more than 30 dB of power leakage in the RF front-end system. From Figure 6(b), it is illustrated that the simulated return loss of the ON-state port (S_{11}) was 12 dB. In addition, during the Tx mode operation, the absorptive property of the FIS can be observed at the OFF-state port (Port 2), where the simulated and measured return losses (S_{22}) are more than 12 dB as illustrated in Figure 6(c). Figure 6(d) shows that the proposed T-shape FIS achieved very low insertion loss. The simulated result of the insertion loss S_{13} was 4 dB, while the measured S_{13} was about 2.3 dB. The slight difference between simulated and measured results was due to the coupling between even- and odd-modes. The band-stop response of the switchable T-shape resonator helped to improve the isolation of the FIS, while the bandpass response represented the insertion loss of the FIS design. In addition, very high-power handling of SPDT switch can be achieved during ON state where the $P_{1\,\mathrm{dB}}$ of the PIN diodes is greater than 40 dBm [31]. Table 3 summarizes the simulation and measurement results of the absorptive filter-integrated switch using T-shape resonator.

Table 4 is a comparison between this work and ten of the most related previous studies. All of them shared the same integration device and integrated a bandpass filter (BPF) with an SPDT switch. For the switching element, PIN diodes were utilised in most research works. To integrate BPF with SPDT switch in a one device, several techniques were used such as dielectric resonators (DRs) [15], LC resonators [11], SISL [30], and common shorted stepped-impedance resonator (CSSIR) [25]. While the output of the first nine listed studies depicted low insertion and high isolation, they suffered from low return loss at OFF-port; in other words, they did not provide an absorptive feature as created in [25]. However, the FIS in [25] has been designed to support a lower frequency application (1 GHz) using CSSIR with a higher number of PIN diodes than that utilised in this work.

Table 3. The simulation and measurement results of the FIS.

FIS	S_{11}	S_{22}	S_{12}	S_{13}
Simulation	13	12	38	4
Measurement	13	14	32	2

Table 4. A comparison between this work and the related studies.

Ref.	Integration	Technique	Switching Element	Frequency (GHz)	IL (dB)	Iso (dB)	Absorptive?	BW @ OFF-port (MHz)
[5]	BPF-DPDT	Hairpin resonators	PIN diodes	1.5	3.1	43	No	NA
[9]	BPF-SPDT	Coupled lines	PIN diodes	9.4	2.4	30	No	NA
[16]	BPF-SPDT	Multi-coupled line	PIN diodes	1	0.97	20	No	NA
[22]	BPF-SPDT	Coupled lines	HEMT	42	3.5	29	No	NA
[13]	BPF-SPDT	DR & Cavity	PIN diodes	1.832	0.4	45	No	NA
[11]	BPF-SPDT	LC resonators	PIN diodes	1	2.8	41	No	NA
[14]	BPF-SPST	SiGe BiCMOS		24/60	2.9	43	No	NA
[15]	BPF-SPDT	DR	PIN diodes	1.86	0.5	40	No	NA
[30]	BPF-SPDT	SISL	PIN diodes	1	1.57	40	No	NA
[25]	BPF-SPDT	CSSIR	8 PIN diodes	1	1.99	58.9	Yes	100
This Work	BPF-SPDT	Absorptive T-shape resonator	6 PIN diodes	2.45 GHz	4.0	30.6	Yes	180

6. CONCLUSION

The proposed absorptive filter-integrated SPDT switch with switchable T-shape resonators was designed and mathematically analysed for 2.45 GHz applications. The theory of matched band-stop filter was shortly discussed and then applied in filter-integrated SPDT switch design. The switchable T-shape resonators could be reconfigured between band-stop and bandpass filter responses. The proposed design was successfully simulated in the ADS software. More than 30 dB isolations, greater than 10 dB return loss at used and unused ports, and low insertion loss were observed in the measured results. The proposed design had an absorptive feature, which was effective for applications that required good VSWR for all operating ports. The absorptive filter-integrated SPDT switch could mitigate the problems of multiple internal reflections existing in the RF front end, which can reduce the effect of microwave switch on the RF front end performance.

ACKNOWLEDGMENT

We would like to thank Universiti Teknikal Malaysia Melaka (UTeM) Zamalah Scheme for the support to publish this paper. Additionally, thanks go to the Center for Research and Innovation Management (CRIM) and Centre for Telecommunication Research & Innovation (CeTRI) for their encouragement and motivation to conduct this research work.

REFERENCES

1. Ham, J., et al., "CMOS power amplifier integrated circuit with dual-mode supply modulator for mobile terminals," *IEEE Transactions on Circuits and Systems I: Regular Papers*, Vol. 63, No. 1, 157–167, 2016.
2. Singh, R., et al., "A 3/5 GHz reconfigurable CMOS low-noise amplifier integrated with a four-terminal phase-change RF switch," *2015 IEEE International Electron Devices Meeting (IEDM)*, IEEE, 2015.
3. Reyaz, S., et al., "A W band RFMEMS switched LNA in a 70 nm mHEMT process," *International Journal of RF and Microwave ComputerAided Engineering*, Vol. 25, No. 7, 639–646, 2015.
4. Sahoo, A. K., R. D. Gupta, and M. S. Parihar, "A 2×2 integrated filter antenna array," *2017 11th European Conference on Antennas and Propagation (EUCAP)*, IEEE, 2017.
5. Chao, S. F. and M. W. Shih, "Design of double-pole-double-throw bandpass filter-integrated switches," *PIERS Proceedings*, 1241–1244, Kuala Lumpur, Malaysia, March 27–30, 2012.
6. Lee, J., Z.-M. Tsai, and H. Wang, "A band-pass filter-integrated switch using field-effect transistors and its power analysis," *2006 IEEE MTT-S International Microwave Symposium Digest*, IEEE, 2006.
7. Lee, D. and C. Nguyen, "K/Ka-band single-pole single-throw switch with integrated filtering function," *2014 IEEE Antennas and Propagation Society International Symposium (APSURSI)*, IEEE, 2014.
8. Liao, W.-H., C.-S. Chen, and Y.-S. Lin, "Single-chip integration of electronically switchable bandpass filter for 3.5 GHz WiMAX application," *2010 IEEE MTT-S International Microwave Symposium*, IEEE, 2010.
9. Rave, C., F. O. Storjohann, and A. F. Jacob, "A compact bandpass filter integrated SPDT PIN switch at X-band," *GeMiC 2014, German Microwave Conference*, VDE, 2014.
10. Lee, J., et al., "Low insertion-loss single-pole–double-throw reduced-size quarter-wavelength HEMT bandpass filter integrated switches," *IEEE Transactions on Microwave Theory and Techniques*, Vol. 56, No. 12, 3028–3038, 2008.
11. Xu, J., et al., "Quasi-lumped-element filter-integrated single-pole double-throw switch," *IEEE Transactions on Microwave Theory and Techniques*, Vol. 65, No. 11, 4564–4571, 2017.
12. Chao, S.-F., et al., "40-GHz MMIC SPDT and multiple-port bandpass filter-integrated switches," *IEEE Transactions on Microwave Theory and Techniques*, Vol. 55, No. 12, 2691–2699, 2007.

13. Zhang, X. Y., J.-X. Xu, and J.-X. Chen, "High-power filtering switch with low loss and high isolation based on dielectric resonator," *IEEE Transactions on Microwave Theory and Techniques*, Vol. 65, No. 6, 2101–2110, 2017.
14. Um, Y. and C. Nguyen, "High-isolation multimode multifunction 24-/60-GHz CMOS dual-bandpass filtering T/R switch," *IEEE Microwave and Wireless Components Letters*, Vol. 28, No. 8, 696–698, 2018.
15. Xu, J.-X., et al., "Narrowband single-pole double-throw filtering switch based on dielectric resonator," *IEEE Microwave and Wireless Components Letters*, Vol. 28, No. 7, 594–596, 2018.
16. Chen, C.-S., J.-F. Wu, and Y.-S. Lin, "Compact single-pole-double-throw switchable bandpass filter based on multicoupled line," *IEEE Microwave and Wireless Components Letters*, Vol. 24, No. 2, 87–89, 2013.
17. Chao, S.-F., et al., "Electronically switchable bandpass filters using loaded stepped-impedance resonators," *IEEE Transactions on Microwave Theory and Techniques*, Vol. 54, No. 12, 4193–4201, 2006.
18. Chao, S.-F., et al., "A 40-GHz MMIC SPDT bandpass filter integrated switch," *2007 IEEE/MTT-S International Microwave Symposium*, IEEE, 2007.
19. Tsai, Z.-M., et al., "Analysis and design of bandpass single-pole-double-throw FET filter-integrated switches," *IEEE Transactions on Microwave Theory and Techniques*, Vol. 55, No. 8, 1601–1610, 2007.
20. Lee, J., et al., "A Q-band low loss reduced-size filter-integrated SPDT switch using 0.15 μm MHEMT technology," *2008 IEEE MTT-S International Microwave Symposium Digest*, IEEE, 2008.
21. Phudpong, P., et al., "A high-isolation low-insertion-loss filter-integrated PIN diode antenna switch," *2009 Asia Pacific Microwave Conference*, IEEE, 2009.
22. Chao, S.-F., "42 GHz MMIC SPDT bandpass filter-integrated switch using HEMT loaded coupled lines," *Electronics Letters*, Vol. 48, No. 9, 505–506, 2012.
23. Phudpong, R., et al., "An absorptive bandpass-integrated p-i-n diode T/R switch for 2.5 GHz WiMAX high power terminals," *Microwave and Optical Technology Letters*, Vol. 54, No. 12, 2705–2708, 2012.
24. Xu, J., Z. Y. Chen, and Q. H. Cai, "Miniaturized frequency-agile bandpass filter integrated single-pole double-throw switch," *International Journal of RF and Microwave Computer-Aided Engineering*, Vol. 28, No. 8, e21403, 2018.
25. Xu, J., H. Wan, and Z.-Y. Chen, "Sharp skirt bandpass filter-integrated single-pole double-throw switch with absorptive OFF-state," *IEEE Transactions on Microwave Theory and Techniques*, Vol. 67, No. 2, 704–711, 2018.
26. Guyette, A. C., et al., "Perfectly-matched bandstop filters using lossy resonators," *IEEE MTT-S International Microwave Symposium Digest, 2005*, IEEE, 2005.
27. Pozar, D. M., *Microwave Engineering*, John Wiley & Sons, 2009.
28. Hunter, I., *Theory and Design of Microwave Filters*, No. 48, IET, 2001.
29. Adoum, B. A., W. P. Wen, and M. S. Osman, "Switchable matched band-stop filter for high power interference mitigation," *2013 Asia-Pacific Microwave Conference Proceedings (APMC)*, IEEE, 2013.
30. Ma, K., et al., "A novel compact self-packaged SPDT switchable BPFs based on SISL platform," *IEEE Transactions on Industrial Electronics*, Vol. 66, No. 9, 7239–7249, 2018.
31. SolutionsNXP, "AN11991 Application note," 1–61, accessible at: https://www.nxp.com/docs/en-/application-note/AN11991.pdf, 2017.

Erratum to "Absorptive Filter Integrated Single Pole Double Throw Switch Using Switchable T-Shape Resonator for IoT Applications"

by Abdullah M. Zobilah, Noor A. Shairi, Zahriladha Zakaria, Peng W. Wong, Mohd K. Zahari, Mohammed Y. Algumaei, and Zayed A. Nasser

in Progress In Electromagnetics Research C, Vol. 103, 167–176, 2020

Abdullah M. Zobilah[1, *], Noor A. Shairi[1], Zahriladha Zakaria[1], Peng W. Wong[2], Mohd K. Zahari[1], Mohammed Y. Algumaei[1], and Zayed A. Nasser[1]

We would like to do a minor correction on the part of the acknowledgment as following.

The Error:

We would like to thank Universiti Teknikal Malaysia Melaka (UTeM) Zamalah Scheme for the support to publish this paper. Additionally, thanks go to the Center for Research and Innovation Management (CRIM) and Centre for Telecommunication Research & Innovation (CeTRI) for their encouragement and motivation to conduct this research work.

The Correction:

We would like to thank Universiti Teknikal Malaysia Melaka (UTeM) Zamalah Scheme for the support to publish this paper.

Received 10 August 2020, Added 11 August 2020
* Corresponding author: Abdullah Mohammed Saghir Zobilah (zobilah12@hotmail.com).
[1] Microwave Research Group (MRG), Centre for Telecommunication Research & Innovation (CeTRI), Fakulti Kejuruteraan Elektronik dan Kejuruteraan Komputer (FKEKK), Universiti Teknikal Malaysia Melaka (UTeM), Hang Tuah Jaya, Durian Tunggal, Melaka 76100, Malaysia. [2] Electrical & Electronic Engineering Department, Universiti Teknologi Petronas (UTP), Bandar Seri Iskandar, Tronoh, Perak 31750, Malaysia.